厚生労働科学研究費補助金

創薬基盤推進研究事業

複数のガン防御機構を標的とした遅発型ガン発症マウスライブラリーの作製とガン予防戦略確立への応用に関する研究

平成２１年度　総括研究報告書

研究代表者　中西　真

平成２２（２０１０）年　３月

目　　次

Ⅰ．総括研究報告
複数のガン防御機構を標的として遅発型ガン発症マウスライブラリーの作製と
ガン予防戦略確立への応用に関する研究 ---------- 1
中西　真

II. 研究成果の刊行に関する一覧表 ---------- 4

III. 研究成果の刊行物・別刷 ---------- 5

厚生労働科学研究費補助金（創薬基盤推進研究事業）
（総括）研究報告書

複数のガン防御機構を標的とした遅発型ガン発症マウスライブラリーの作製とガン予防戦略確立への応用に関する研究

研究代表者　中西　真　名古屋市立大学大学院医学研究科教授

研究要旨：ガン防御機構を制御するシステムの二重、三重変異マウスを作製し、臨床で見られる遅発型ガン発症マウスライブラリーを確立して、ガン予防戦略確立に有益であることを明らかにする。

研究分担者　なし

A. 研究目的

現在までにp53等のガン抑制遺伝子変異マウスが高率にガンを発症することが知られている。しかしながら、ヒト臨床ガンに見られるこれらガン抑制遺伝子の変異は、ガン発症の原因ではなく、むしろガン悪性化の原因か、あるいはガン進展の結果であると考えられている。実際、これらガン抑制遺伝子のノックアウトマウスは生後まもなく早期にガンを発症し、そのガンの種類もヒトの多くの臨床ガンとは大きく異なる特徴を示す。臨床ガンにおいてはチェックポイント、アポトーシス、細胞老化等の複数のガン防御機構に機能不全が蓄積することが初発原因と考えられている。これらを踏まえて、本研究ではガン防御機構を制御するシステムの二重、三重変異マウスを作製し、遅発型臨床ガン発症マウスライブラリーを確立して、ガン予防戦略確立に有益であることを明らかにする。

B. 研究方法

本研究は、研究代表者（中西真）と代表者の研究室に所属する２名の連携研究者（丹伊田浩行助教、島田緑特任助教）により、名古屋市立大学大学院医学研究科細胞生化学教室と実験動物センターを中心に行われた。平成２１年度は、Chk1/Chk2二重変異マウスの遅発型発ガンの原因解析と、新たなガン防御機構の解明、さらにはTip60, mdm2, p27等の変異マウスを用いた新たな遅発型ガン発症モデルマウスの作製を行った。具体的には、

1. Chk1/Chk2二重変異マウス由来のプライマリー胎児繊維芽細胞（MEFs）を用いて、DNA損傷に反応したG1/S期、およびG2/M期細胞周期停止機能を解析した。同時にDNA損傷に反応したDNA合成抑制についても明らかにした。また、DNA損傷修復能、アポトーシス誘導能、癌遺伝子誘導早期老化、高複製刺激誘導細胞老化、DNA損傷誘導早期細胞老化能を明らかにした。
2. 新たな発ガン防御機構として、DNA修復過程における適切なdNTPsを供給する機構を明らかにする目的で、RNRに結合するタンパク質のスクリーニングを行い、Tip60を同定するとともに、これら複合体の性質を明らかにした。
3. チェックポイント不全およびアポトーシス亢進と、DNA損傷部位へのdNTPs供給に不全を示す$Tip60^{+/-}Chk1^{+/-}$, $Tip60^{+/-}mdm2^{C462A}$, アポトーシス亢進とチェックポイントに不全を示す$mdm2^{C462A}Chk1^{+/-}$マウス、さらにはG1チェックポイントとアポトーシス不全に関与する$p27^{-/-}Chk1^{+/-}$マウスを作製する目的で、これら変異マウスの交配を行った。

（倫理面での配慮）

ノックアウトマウス作成、およびマウスの機能解析、発ガン実験に関しては、すべて名古屋市立大学医学研究科において規定された実験動物指針に基づいて行った。また適宜、厚生労働省指導の所管する実施機関における動物実験等の実施に関する基本指針を参考とし、実験動物に与える苦痛、およびストレスを必要最低限にした。本研究における組み換え実験についても名古屋市立大学医学研究科組み換え実験委員会での承認を得て、実験指針に基づいて行われた。また本研究は名古屋市立大学利益相反委員会において利益相反には該当しないと判定された。

C. 研究結果

本研究の最終目標は、ヒト型遅発性ガン発症モデルマウスライブラリーを作製することにある。平成２１年度はChk1/Chk2二重変異マウスで見られる高発ガン性の原因を明らかにする目的で、マウス胎児繊維芽細胞の解析を行った。Chk1ヘテロ欠失変異は、細胞周期チェックポイント異常、とりわけDNA損傷に反応したG2/M期停止の部分異常を示した。一方、Chk2の完全欠失はDNA損傷に反応したアポトーシス誘導不全をきたすことが明らかとなった。Chk2完全欠失はDNA損傷修復異常も示した。DNA損傷に反応したG1/S期停止には、Chk1およびChk2の両方が協調的に機能していることが分かった。しかしながら、発ガン防御に重要な役割を果たしているDNA損傷に反応した早期細胞老化誘導は$Chk1^{+/-}Chk2^{-/-}$マウスの胎児繊維芽細胞で維持されていた。

さらに、新たな発ガン防御機構として、DNA修復過程における適切なdNTPsを供給する機構を同定した。細胞内dNTPs濃度の制御は染色体DNAの安定維持に重要であると考えられていたが、dNTPs供給の律速酵素であるリボヌクレオチド還元酵素（RNR）がTip60ヒストンアセチル化酵素依存的にDNA損傷部位に集積することを明らかにした。さらに、損傷部位へのRNRの集積が効率的なDNA損傷修復に必須であることを明らかにした。

一方、新たな遅発型ガン発症モデルマウスを作製する目的で、チェックポイント不全およびアポトーシス亢進と、DNA損傷部位へのdNTPs供給に不全を示す$Tip60^{+/-}Chk1^{+/-}$, $Tip60^{+/-}mdm2^{C462A}$, アポトーシス亢進とチェックポイントに不全を示す$mdm2^{C462A}Chk1^{+/-}$マウス、さらにはG1チェックポイントとアポトーシス不全に関与する$p27^{-/-}Chk1^{+/-}$マウスを作製し発がん解析を行っている。

D. 考察

$Chk1^{+/-}Chk2^{-/-}$二重変異マウスは、早期細胞老化以外のDNA損傷反応を介した細胞応答における異常の結果、遅発型ガン発症を示した。実際、これら二重変異マウスから得られた胎児繊維芽細胞では高率に染色体異常を認めた。これらの結果は、ヒトに見られる発ガンはガン防御機構のうちある程度正常に機能する機構が残存するために、ガン発症に時間を要するのではないかと推察された。一方、新たなガン防御機構の解明は、新規のガン治療・予防戦略の確立に道を拓くものと期待される。とりわけ、核内におけるdNTPsの濃度調節が変異率やDNA修復能に大きな影響を与えるという知見は、DNA修復機構の詳細な解明に大きく寄与するのみならず、外的に細胞内dNTPs濃度を制御することを可能にすれば、ガン発症を予防できる可能性を示唆しており、本研究の最終年度において解析していく予定である。さらに、これらの知見をもとに新たに4種類の二重変異マウスを作製し、ヒト型遅発性ガン発症モデルマウスをして有益かどうかについて検証し、その分子基盤を明らかにすることは、発ガン機構の解明にもつながるものと予想され、非常に興味深い。

E. 結論

$Chk1^{+/-}Chk2^{-/-}$および$Chk1^{+/-}Chk2^{+/-}$二重変異マウスは、DNA 損傷に反応した一過性細胞周期停止、およびアポトーシス誘導に重複した部分不全を持つマウスであり、ヒトに見られるガン発症と同様に遅発性にガンを発症した。さらに、dNTPs 合成の律速酵素である RNR が Tip60 ヒストンアセチル化酵素と直接結合して複合体を形成し、DNA 損傷部位へ適切な dNTPs を供給していることを明らかにした。この供給機構に不備があると細胞周期での G1 期での DNA 修復に異常をきたすことも明らかにした。

F. 健康危機情報

特にない。

G. 研究発表

1. 論文発表

Niida, H., Katsuno, Y., Sengoku, M., Shimada, M., Yukawa, M., Ikura, M., Ikura, T., Kohno, K., Shima, H., Suzuki, H., Tashiro, S., and Nakanishi, M. Essential role of Tip60-dependent recruitment of ribonucleotide reductase at DNA damage sites in DNA repair during G1 phase. ***Genes and Dev.*** 24, 333-338 (2010)

Ohoka, N., Sakai, S., Onozaki, K., Nakanishi, M., and Hayashi, H. Anaphase promoting complex/cyclosome-cdh1 mediates the ubiquitination and degradation of TRB3. ***Biochem. Biophys. Res. Commun.*** 392, 289-294 (2010)

Nakanishi, M., Katsuno, Y., Niida, H., Murakami, H., and Shimada, M. Chk1-cycline A/Cdk1 axis regulates origin firing programs in mammals. ***Chromosomal Res.*** 18, 103-113 (2010)

Nakanishi, M., Niida, H., Murakami, H., and Shimada, M. DNA damage responses in skin biology-Implications in tumor prevention and aging acceleration. ***J Dermatol Sci.*** 56, 76-81 (2009)

Shimada,M.,Yamamoto,A., Murakami-Tonami, Y., Nakanishi, M., Yoshida, T., Aiba, H., and Murakami, H. Casein kinase II is required for the spindle assembly checkpoint by regulating Mad2p in fission yeast. ***Biochem. Biophys. Res. Commun.*** 388, 529-532 (2009)

Zineldeen, D.H., Shimada, M., Niida, H., Katsuno, Y., and Nakanishi, M. Ptpcd-1 is a novel cell cycle related phosphatase that regulates centriole duplication and cytokinesis. ***Biochem. Biophys. Res. Commun.*** 380, 460-466 (2009)

２．学会発表

中西　真
「DNA 損傷部位への適切な dNTP 供給機構」
平成２１年１０月２日
第６８回日本癌学会学術総会

G．知的財産権の出願・登録状況（予定を含む）

１．特許取得　なし

２．実用新案登録　なし

３．その他　なし

書籍

著者氏名	論文タイトル名	書籍全体の編集者名	書　籍　名	出版社名	出版地	出版年	ページ

雑誌

発表者氏名	論文タイトル名	発表誌名	巻号	ページ	出版年
Niida, H., Katsuno, Y., Sengoku, M., Shimada, M., Yukawa, M., Ikura, M., Ikura, T., Kohno, K., Shima, H., Suzuki, H., Tashiro, S., and Nakanishi, M.	Essential role of Tip60-dependent recruitment of ribonucleotide reductase at DNA damage sites in DNA repair during G1 phase.	***Genes and Dev.***	24	333-338	2010
Ohoka, N., Sakai, S., Onozaki, K., Nakanishi, M., and Hayashi, H.	Anaphase promoting complex/cyclosome-cdh1 mediates the ubiquitination and degradation of TRB3.	***Biochem. Biophys. Res. Commun.***	392	289-294	2010
Nakanishi, M., Katsuno, Y., Niida, H., Murakami, H., and Shimada, M.	Chk1-cycline A/Cdk1 axis regulates origin firing programs in mammals.	***Chromosomal Res.***	18	103-113	2010
Nakanishi, M., Niida, H., Murakami, H., and Shimada, M.	DNA damage responses in skin biology-Implications in tumor prevention and aging acceleration.	***J Dermatol Sci.***	56	76-81	2009
Shimada,M.,Yamamoto,A., Murakami-Tonami, Y., Nakanishi, M., Yoshida, T., Aiba, H., and Murakami, H.	Casein kinase II is required for the spindle assembly checkpoint by regulating Mad2p in fission yeast.	***Biochem. Biophys. Res. Commun.***	388	529-532	2009
Zineldeen, D.H., Shimada, M., Niida, H., Katsuno, Y., and Nakanishi, M.	Ptpcd-1 is a novel cell cycle related phosphatase that regulates centriole duplication and cytokinesis.	***Biochem. Biophys. Res. Commun.***	380	460-466	2009

Essential role of Tip60-dependent recruitment of ribonucleotide reductase at DNA damage sites in DNA repair during G1 phase

Hiroyuki Niida,[1] Yuko Katsuno,[1] Misuzu Sengoku,[1] Midori Shimada,[1] Megumi Yukawa,[1] Masae Ikura,[2] Tsuyoshi Ikura,[2] Kazuteru Kohno,[3] Hiroki Shima,[3] Hidekazu Suzuki,[3] Satoshi Tashiro,[3] and Makoto Nakanishi[1,4]

[1]Department of Cell Biology, Graduate School of Medical Sciences, Nagoya City University Medical School, Nagoya 467-8601, Japan; [2]Radiation Biology Center, Kyoto University, Kyoto 606-8501, Japan; [3]Department of Cell Biology, Research Institute for Radiation Biology and Medicine (RIRBM), Hiroshima University, Hiroshima 734-8553, Japan

A balanced deoxyribonucleotide (dNTP) supply is essential for DNA repair. Here, we found that ribonucleotide reductase (RNR) subunits RRM1 and RRM2 accumulated very rapidly at damage sites. RRM1 bound physically to Tip60. Chromatin immunoprecipitation analyses of cells with an I-SceI cassette revealed that RRM1 bound to a damage site in a Tip60-dependent manner. Active RRM1 mutants lacking Tip60 binding failed to rescue an impaired DNA repair in RRM1-depleted G1-phase cells. Inhibition of RNR recruitment by an RRM1 C-terminal fragment sensitized cells to DNA damage. We propose that Tip60-dependent recruitment of RNR plays an essential role in dNTP supply for DNA repair.

Supplemental material is available at http://www.genesdev.org.

Received September 15, 2009; revised version accepted December 22, 2009.

Maintenance of the optimal intracellular concentrations of deoxyribonucleotides (dNTPs) is critical not only for faithful DNA synthesis during DNA replication and repair, but also for the survival of all organisms. Ribonucleotide reductase (RNR), composed of a tetrameric complex of two large catalytic (RRM1) subunits and two small subunits (RRM2 or 53R2), catalyzes de novo synthesis of dNTPs from the corresponding ribonucleotides (Reichard 1993). This reaction is the rate-limiting process in DNA precursor synthesis and is regulated by multiple complex mechanisms, including transcriptional and subcellular localization regulation of RNR (Nordlund and Reichard 2006). In order to duplicate their chromosomal DNA, mammalian S-phase cells possess 15–20 times more dNTP pools than resting quiescent cells, whereas whole dNTP pools were almost unchanged after DNA damage, suggesting the presence of a unique mechanism that supplies a sufficient quantity of dNTPs at repair sites (Hakansson et al. 2006). DNA synthesis must function properly in both repair and replication (dNTP concentrations in fibroblasts were estimated to be as follows: ~0.5 μM in G0/G1-phase cells, and ~10 μM in S-phase cells, given that the average volume of a fibroblast is 3.4 pL) (Imaizumi et al. 1996). Although the amount of dNTPs required for DNA repair is small, their concentration during DNA synthesis is critical because DNA polymerase involved in DNA repair (Kraynov et al. 2000; Johnson et al. 2003) has similar kinetic affinities for dNTPs (~10 μM) to those involved in DNA replication (~10 μM) (Dong and Wang 1995). Therefore, the dNTPs might be compartmentalized close to the damage sites during the DNA repair process. In this study, we show that, in mammals, both RRM1 and RRM2 rapidly accumulated at double-strand break (DSB) sites in a Tip60-binding-dependent manner.

[*Keywords*: DNA repair; ribonucleotide reductase; Tip60; dNTPs; genomic instability; DNA double-strand breaks]
[4]**Corresponding author.**
E-MAIL mkt-naka@med.nagoya-cu.ac.jp, FAX 81-52-842-3955.
Article is online at http://www.genesdev.org/cgi/doi/10.1101/gad.1863810.

Results and Discussion

In order to understand the mechanisms by which dNTPs are sufficiently supplied at DNA damage sites in mammals, we first examined changes in the subcellular localization of RRM1 and RRM2 subunits after ionizing irradiation (IR) irradiation. Although both RRM1 and RRM2 predominantly localized in the cytoplasm as reported previously (Pontarin et al. 2008), we also detected trace, but significant, signals of both proteins in chromatin fraction (see Fig. 1C; Supplemental Fig. S4A–D). After removing soluble RNR proteins by detergent extraction, we found that RRM1 and RRM2 proteins formed nuclear foci that colocalized with γH2AX (Fig. 1A). RRM1 nuclear foci were not evident without DNA damage (Supplemental Fig. S1A) or after RRM1 depletion by siRNA (Supplemental Fig. S1B). Ultravioulet A (UVA) microirradiation resulted in the accumulation of RRM1 and RRM2 along microirradiated lines as early as 5 min after treatment (Fig. 1B). These accumulations were also observed when cells were not subjected to detergent extraction or preincubation with BrdU (Supplemental Fig. S2A,B), but were significantly compromised when R1 expression was knockdown by siRNA (Supplemental Figs. S2C, S4B), excluding the possibility that accumulated signals at DSB sites were artifacts during cell-staining processes. These results indicated that RNR, at least in part, was rapidly recruited to DSB sites.

In order to determine the molecular basis underlying RNR recruitment at the sites of DSBs, we performed yeast two-hybrid screening using RRM1 as a bait. Of a total of 5×10^6 transformants from a HeLa cell cDNA library, 45 positive colonies were confirmed to be lacZ-positive. They contained overlapping cDNAs derived from three genes: *RRM2* and *53R2* (both encoding a small subunit of RNR), and another encoding *Tip60* histone acetyltransferase (Tip60). Small C-terminal RRM1 deletion mutants (Δ761-C and Δ781-C) failed to bind Tip60, but retained the ability to bind to RRM2 (Supplemental Fig. S3A). In contrast, the N-terminal truncation mutant of Tip60

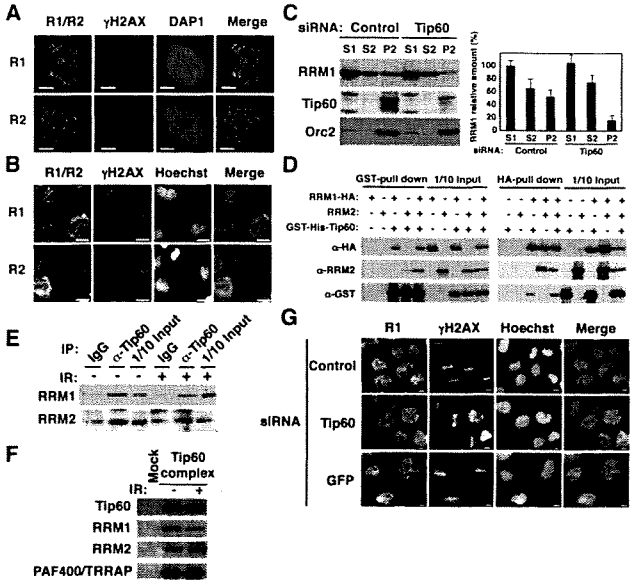

Figure 1. Tip60-dependent recruitment of RNR at DSB sites. (*A*) HeLa cells were exposed to IR at 1 Gy, subjected to in situ detergent extraction after 5 min, and immunostained with the indicated antibodies. Bars, 5 μm. (*B*) GM02063 cells were subjected to UVA microirradiation and immunostained with the indicated antibodies after 5 min. RRM1 or RRM2 and γH2AX signals are shown in green and red, respectively, in merged images. Bars, 10 μm. (*C*) IR-irradiated HeLa cell lysates treated with the indicated siRNAs were fractionated as described in the Materials and Methods. (*Left* panels) The fractions were subjected to immunoblotting using the indicated antibodies. (*Right* panel) The RRM1 bands were quantitated, and the results are presented as percentages of S1 fraction. Data are mean ± standard deviation (n = 3). (*D*) Sf9 lysates expressing RRM1-HA, RRM2, or GST-His-Tip60 were subjected to GST pull-down or HA pull-down assays using the indicated antibodies. (*E*) Chromatin fractions from IR- or mock-treated HeLa cells (after 5 min) were solubilized with micrococcal nuclease. The solubilized extracts were immunoprecipitated with anti-Tip60 antibodies or control IgG. The resulting precipitates and a 10% input (1/10 Input) were immunoblotted with the indicated antibodies. (*F*) The affinity-purified Tip60 complexes, as described in the Materials and Methods, were subjected to immunoblotting using the indicated antibodies. (*G*) GM02063 cells were treated with control, Tip60, or GFP siRNAs and then subjected to UVA microirradiation as in *B*.

(TC2) could interact with RRM1, but no mutant with any additional truncation of TC2 was able to do so (Supplemental Fig. S3B). Full-length Tip60 failed to bind full-length RRM2 (Supplemental Fig. S3C). We generated the C-terminal fragment of RRM1 (amino acids 701–792) with a SV40 nuclear localization signal (NLS-RC1-HA) and examined its ability to bind Tip60 in vivo and in vitro. NLS-RC1-HA, but not a control NL-GFP-HA fragment, was detected in the anti-Myc immunoprecipitates when transiently coexpressed with Tip60-Myc (Supplemental Fig. S3D). Purified MBP-fused RC1 produced in *Escherichia coli* was capable of binding to GST-Tip60 expressed in insect cells (Supplemental Fig. S3E). Both Δ761-C and Δ781-C failed to bind chromatin, further confirming that the binding of RRM1 to chromatin required its interaction with Tip60 (Supplemental Fig. S3F).

Similarly to Chk1 (Niida et al. 2007; Shimada et al. 2008), endogenous RRM1 was present in cytosolic (S1), nucleoplasmic (S2), and chromatin-bound (P2) fractions (Supplemental Fig. S4A). Tip60 existed predominantly in the chromatin-bound fraction (P2). Both RRM1 and Tip60 proteins in this fraction were partly solubilized by treatment with micrococcal nuclease (Mnase), suggesting that they associated with chromatin. RRM1 knockdown showed a significant decrease of RRM1 protein levels in both soluble and chromatin-bound fractions (Supplemental Fig. S4B). IKKα and Orc2 were detected predominantly in soluble and chromatin fractions, respectively, indicating that cell fractionation was done successfully. Ectopic RRM1-HA present in the chromatin fraction was increased when Tip60-Myc-His was coexpressed, although a low level of RRM1-HA was detected in the absence of Tip60-Myc-His, presumably due to the presence of endogenous Tip60 (Supplemental Fig. S4C). The amounts of RRM1 and Tip60 bound to the chromatin were not affected by DNA damage (Supplemental Fig. S4D). However, depletion of Tip60 resulted in a reduction in the amount of RRM1 on chromatin (Fig. 1C). Taken together, chromatin binding of RRM1 appeared to be Tip60-dependent. RRM1-HA, but not the RRM2 subunit alone, formed a complex with GST-His-Tip60 in insect cells (Fig. 1D, left panels). RRM2 also formed a complex with GST-His-Tip60 in a manner dependent on the presence of RRM1-HA. Consistently, accumulation of RRM2 at DSB sites was compromised when RRM1 was depleted (Supplemental Fig. S2D). Immunoprecipitations using anti-HA antibodies demonstrated that RRM1-HA bound to both RRM2 and GST-His-Tip60 (Fig. 1D, right panels). RRM1 and RRM2 were detected in the precipitates of anti-Tip60 antibodies from the solubilized chromatin, even in the absence of DNA damage (Fig. 1E). To further confirm the interaction between RNR and Tip60, we purified the Tip60 complex from HeLa cell nuclear extracts expressing Flag-HA Tip60 as reported previously (Ikura et al. 2000, 2007). RRM1 and RRM2, as well as PAF400/TRRAP as a positive control (Murr et al. 2006), were detected in Tip60 complex from extracts with or without DNA damage (Fig. 1F). Tip60 knockdown by siRNA or shRNA abrogated accumulation of RRM1 along with microirradiated lines (Fig. 1G; Supplemental Fig. S2E). These results suggested that RRM1 recruitment at DSB sites was Tip60-dependent.

To determine precisely whether RRM1 was recruited at the site of DNA damage, we generated *Ku*-deficient mouse embryonic fibroblasts (MEFs) in which a single DSB was introduced after infection with adenoviruses expressing I-SceI. This DSB was not rapidly repaired by nonhomologous end-joining, making it easy to detect proteins accumulating at this DSB site by chromatin immunoprecipitation (ChIP) analysis (*STEFKu70*$^{-/-}$*phprt-DR-GFP*) (Fig. 2A; Pierce et al. 2001). Introduction of the DSB was confirmed by Southern blotting (Supplemental Fig. S5). ChIP analyses revealed a substantial increase in the binding of RRM1 as well as Rad51 and Tip60 to a DNA break site. An increase in acetylation of histone H4 was also observed at the damage site (Fig. 2B). These were not seen on infection with control LacZ. Tip60 depletion by two independent siRNAs resulted in a loss of RRM1 binding to a DSB site, as well as a reduction in acetylation of histone H4 (Fig. 2C). A mutant Tip60 lacking histone-acetylating activity could recruit RRM1 to the DSB site similarly to wild-type RRM1 (Supplemental Fig. S6A). Inhibition of ATM, ATR, and DNA-PK by caffeine did not affect RRM1 recruitment (Supplemental Fig. S6B). These results further supported the notion that complex

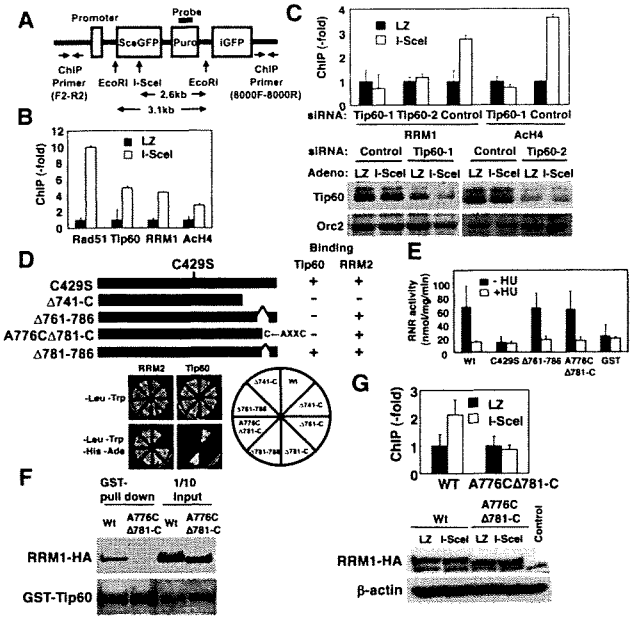

Figure 2. RRM1 is recruited at DSB sites in a Tip60-dependent manner. (*A*) Map of the I-SceI cassette construct containing the I-SceI site, the probe for Southern blotting, and a set of primers for the ChIP assay. (*B*) *STEFKu70*$^{-/-}$*phprt-DR-GFP* cells infected with I-SceI adenoviruses were subjected to ChIP analysis using the indicated antibodies as described in the supporting Materials and Methods. Data are shown as percentages of increases in PCR products from cells expressing I-SceI (I-SceI) relative to those from cells expressing Lac Z (LZ). Data are mean ± standard deviation (n = 3). (*C*) *STEFKu70*$^{-/-}$*phprt-DR-GFP* cells were transfected with two independent Tip60 siRNAs (Tip60-1 and Tip60-2) or control siRNA. ChIP analysis was performed as in *B*. (*Bottom* panels) Aliquots of cell lysates were subjected to immunoblotting using anti-Tip60 antibodies. (*D*) The constructs used are schematically represented, and the specific interaction between RRM1 mutants and Tip60 was assayed using yeast two-hybrid screening. (*E*) An in vitro RNR assay of complexes containing wild-type or various RRM1 mutants was performed as described in the Materials and Methods. (Black bars) −HU; (white bars) +HU (10 mM). Data are mean ± standard deviation (n = 3). (*F*) Sf9 lysates expressing GST-His-Tip60 and the indicated RRM1-HA were subjected to GST pull-down assay using the indicated antibodies. (*G*) Knockout–knock-in *STEFKu70*$^{-/-}$*phprt-DR-GFP* cells expressing wild-type or A776CΔ781-C RRM1-HA were generated by transfection with vectors for either wild-type or A776CΔ781-C RRM1 and then with RRM1 siRNA. Expression vectors of wild type and A776CΔ781-C contain mutations in a specific sequence targeted by siRNA. (*Top* panel) Cells were subjected to ChIP analysis using anti-HA antibodies as in *B*. (*Bottom* panels) Aliquots of cell lysates were subjected to immunoblotting using the indicated antibodies.

formation between RNR and Tip60 is required for recruitment of RNR to sites of DNA damage.

We then examined if RNR recruitment at damage sites was required for effective DNA repair. We first generated RRM1 mutants that lack the ability to bind Tip60 but retain RNR activity. Given that the C-terminal CXXC motif of RRM1 is important for RNR function (Zhang et al. 2007), we constructed *RRM1* mutants containing the CXXC motif but lacking Tip60-binding ability (Δ761–786 and A776CΔ781-C) (Fig. 2D). Wild-type RRM1 or its mutants were coexpressed with RRM2 in insect cells, and the resultant complexes were subjected to an in vitro RNR assay (Fukushima et al. 2001). RNR complexes containing wild-type, Δ761–786, and A776CΔ781-C RRM1 retained hydroxyurea (HU)-sensitive RNR activity (HU is a specific RNR inhibitor), whereas an inactive C429S mutant or GST protein as a negative control did not show RNR activity (Fig. 2E). The specific activity of RNR containing wild-type, Δ761–787, and A776CΔ781-C RRM1 (~50 nmol/mg per minute) was similar to that reported previously (Guittet et al. 2001), confirming the reliability of our results. The A776CΔ781-C mutant failed to form a complex with GST-Tip60 (Fig. 2F). ChIP analysis using RRM1 knockout–knock-in *STEFKu70*$^{-/-}$*phprt-DR-GFP* cells revealed that the A776CΔ781-C mutant failed to accumulate at the DSB site (Fig. 2G). These results indicated that direct interaction of RRM1 to Tip60 is required for triggering its accumulation at the DSB site.

A comet assay revealed that DNA damage in cells was repaired efficiently within 1 h in the absence of HU. However, treatment with HU, and RRM1 or RRM2 depletion, resulted in an impairment of DNA repair (Fig. 3A,B). RNR activity was thus essential for effective repair. Ectopic expression of wild-type *RRM1* with mutations in a specific sequence targeted by siRNA effectively rescued the impaired DNA repair in cells depleted of endogenous RRM1 (Fig. 3C). In contrast, ectopic expression of C429S, Δ761–786, and A776CΔ781-C RRM1 failed

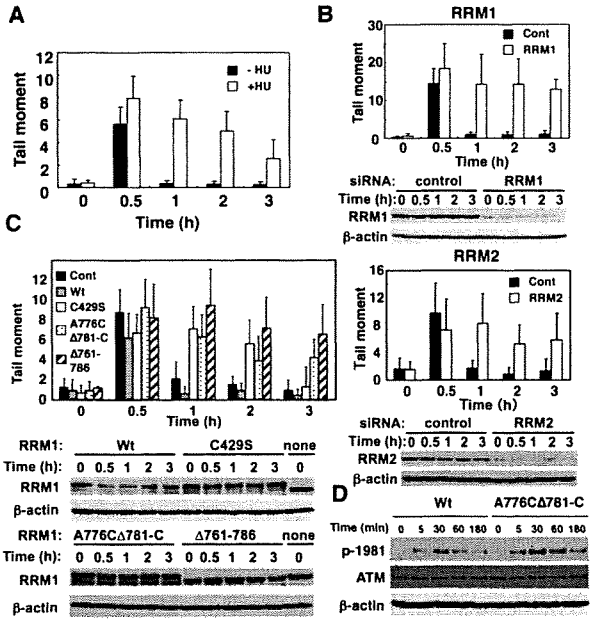

Figure 3. Recruitment of active RNR at DNA damage sites is a prerequisite for effective DNA repair. (*A*) HeLa cells were treated with (open bars) or without (filled bars) 2.5 mM HU, exposed to IR (4 Gy), and subjected to a comet assay as described in the Materials and Methods. The results were obtained by counting at least 50 cells per sample in three independent experiments. (*B*) HeLa cells were transfected with a control (filled bars) or RRM1 or RRM2 siRNA (open bars), and DNA repair was evaluated as in *A*. Cell lysates were subjected to immunoblotting using the indicated antibodies. (*C*) HeLa cells were transfected with or without (filled bars) either wild-type (gray bars), C429S (open bars), A776CΔ781-C (dotted), or Δ761–786 (hatched) RRM1. RRM1-transfected cells were then transfected with RRM1 siRNA. Expression vectors of wild type and various RRM1 mutants contain mutations in a specific sequence targeted by siRNA. DNA repair activity and expression of RRM1 were examined as in *B*. (*D*) Knockout–knock-in HeLa cells expressing wild type or A776CΔ781-C RRM1-HA were exposed to IR, and cell lysates were subjected to immunoblotting as in *C*.

to do so. ATM was activated independently of Tip60 binding to RNR, but this activation was enhanced and prolonged in cells expressing A776CΔ781-C, presumably due to impaired DNA repair (Fig. 3D). It is therefore conceivable that recruitment of active RNR at DNA damage sites is a prerequisite for effective DSB repair, but not for activation of checkpoint signaling. Tip60 is also known to participate in transcriptional regulation of several genes. Neither RRM1 nor RRM2 proteins were affected by Tip60 depletion or overexpression (Supplemental Fig. S7), indicating that the effect of Tip60 did not result from changes in RRM1 and RRM2 expression.

ChIP analyses revealed that NLS-RC1-HA specifically inhibited RRM1 binding, but did not affect Rad51 or Tip60 binding, or increase H4 acetylation at the DSB site in *STEFKu70$^{-/-}$phprt-DR-GFP* cells (Fig. 4A). Expression of NLS-RC1-HA suppressed accumulation of endogenous RRM1 at DNA damage sites (Supplemental Fig. S8A,B), but did not affect the foci formation of 53BP1 at DSB sites (Fig. 4B), or complex formation and activity (Supplemental Fig. S9A,B) of endogenous RNR. However, cells expressing NLS-RC1-HA, but not NLS-GFP-HA, had unrepaired DNA in the tail at 2 h (Fig. 4C). A quantitative colony formation assay was used to examine the DNA damage sensitivity of cells expressing NLS-RC1-HA. Induction of NLS-RC1-HA sensitized cells to IR (Fig. 4D).

Given that levels of dNTP pools are higher during S phase than during G1 phase (Hakansson et al. 2006), recruitment of RNR at damage sites may function at a specific phase of the cell cycle where dNTP pools are low. To address this issue, we synchronized cells at S phase or G1 phase by arrest and release of thymidine or nocodazole, respectively. Recruitment of wild-type RRM1 at a DSB site was observed at both G1 and S phase (Supplemental Fig. S10). However, a comet assay revealed that A776CΔ781-C failed to rescue the impaired DNA repair in RRM1-depleted cells at G1 phase, but not at S phase (Fig. 4E). Consistently, RRM1 mutation of Tip60 binding slightly sensitizes cells to Zeocin (Supplemental Fig. S11A), which causes DNA strand breaks, but not to MMC (Supplemental Fig. S11B), which can cause interstrand cross-linking repaired mainly at S–G2 phase. Intriguingly, this G1-phase-specific impairment of DNA repair was restored when excess amounts of dADP, dGDP, dCDP, and dUMP (250 μM) were supplied in the culture medium (Supplemental Fig. S12). These results suggested that recruitment of RNR was required specifically for effective DNA repair in cells with low levels of dNTPs.

The present study suggests that the RNR recruitment to DSB sites likely provides mechanistic insights into the regulatory events that ensure a balanced supply of dNTPs during mammalian DNA repair. RNR appears to form a complex with Tip60 independently of DNA damage. Thus, it is possible that the RNR–Tip60 complex might have an alternative function, such as regulation of transcription. In response to DNA damage, regulation of the RNR subunit by Wtm1 and Dif1 in budding yeast is radically different in terms of cellular localization (Lee and Elledge 2006; Lee et al. 2008) from that observed in the present study; however, important changes in the subcellular localization of RNR might be conserved. Given that Tip60 is a key regulator of DNA damage responses, the concomitant recruitment of RNR at damage sites suggests the presence of a synthetic regulatory mechanism for DNA repair in mammals.

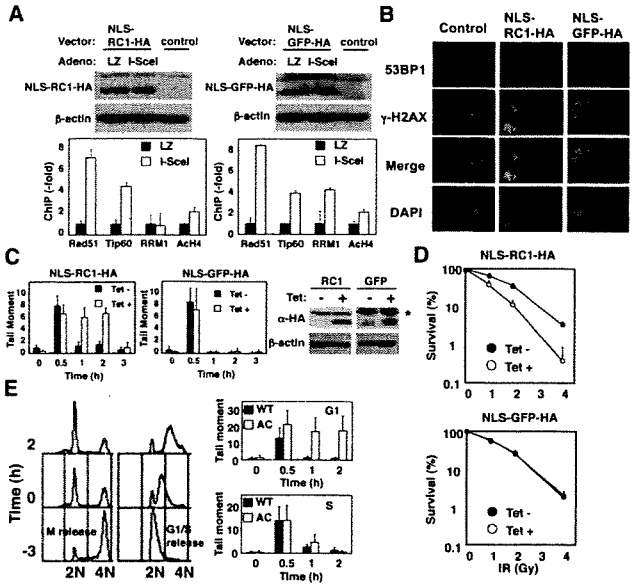

Figure 4. Inhibition of recruitment of RNR at DSB sites by ectopic expression of NLS-RC1-HA abrogates DNA repair and sensitizes cells to DNA damage. (*A*) *STEFKu70$^{-/-}$phprt-DR-GFP* cells expressing NLS-RC1-HA (SV40 NLS-RC1 fragment, 701–792 amino acids) or NLS-GFP-HA (GFP fragment, 1–93 amino acids) were subjected to ChIP analysis as in Figure 2B. (*Top* panels) Cell lysates were subjected to immunoblotting using the indicated antibodies. (*B*, *left* panels) Tet-on HeLa cells expressing NLS-RC1-HA or NLS-GFP-HA were treated with or without tetracycline (1 μg/mL), exposed to IR (4 Gy), and subjected to immunostaining with the indicated antibodies and a comet assay as in Figure 3A. (*Right* panels) IR-untreated lysates were subjected to immunoblotting using the indicated antibodies. (*C*) Asterisk (*) represents nonspecific bands. (*D*) These cells were exposed to the indicated dose of IR, and a quantitative colony formation assay was performed 8 d after treatment. Data are mean ± standard deviation (n = 3). (*E*) Knockout-knock-in HeLa cells expressing either wild-type (filled bars) or A776CΔ781-C (open bars) RRM1-HA were synchronized as described in the Materials and Methods. Synchronized cells were then released into G1 phase or S phase (time −3) and exposed to IR (4 Gy) 3 h after release (time 0). (*Right* panels) DNA repair was evaluated as in *A*. (*Left* panels) Cell cycle distributions are presented.

Materials and methods

Antibodies

Antibodies used were as follows: α-Rad51 (Ab-1, Oncogene Research Products), α-RRM1 (sc-11733 and sc-11731, Santa Cruz Biotechnologies), α-HA (11 666 606 001, Roche Applied Sciences; and PM002, MBL), α-Myc (sc-40 and sc-789, Santa Cruz Biotechnologies), α-RRM2(sc-10844, Santa Cruz Biotechnologies), α-GST (sc-459, Santa Cruz Biotechnologies), α-Chk1 (sc-8408, Santa Cruz Biotechnologies), α-IKKα (sc-7182, Santa Cruz Biotechnologies), α-Orc2 (sc-13238, Santa Cruz Biotechnologies), α-ATM (sc-23921, Santa Cruz Biotechnologies), α-ATMp1981 (no. 4526, Cell Signaling), α-acetylated histone H4 (no. 06-866, Upstate Biotechnologies), and α-phospho-histone H2AX (411-pc-020, TREVIGEN; and 05-636, Upstate Biotechnologies). Anti-Tip60 rabbit polyclonal antibodies were generated by immunization with recombinant GST-His-Tip60 produced in insect cells, and the serum obtained was affinity-purified using a GST-His-Tip60 column.

Two-hybrid interaction assays

The *pGBKT7-RRM1* plasmid was generated by insertion of the full-length human *RRM1*-encoding sequence. *pGBKT7-RRM1* was transformed into

the yeast strain AH101 and mated with yeast Y187 pretransformed with a HeLa cell cDNA library (BD Biosciences). The deletion mutants of RRM1 and Tip60 were amplified by PCR using specific sets of primers. Primer sequences are supplied in the Supplemental Material.

Affinity purification of Tip60 complex

Affinity purification of Tip60 complex was performed as described previously (Ikura et al. 2000, 2007). For the induction of DNA damage, cells were γ-irradiated (12 Gy) after centrifugation.

In situ detergent extraction and immunofluorescence analysis

Immunofluorescence on paraformaldehyde-fixed cells was performed according to a previous report (Green and Almouzni 2003), using the indicated antibodies.

Microirradiation

Microirradiation was performed as described previously (Ikura et al. 2007). In brief, GM02063 cells were maintained on the microscope stage in a Chamlide TC live-cell chamber system (Live Cell Instrument) at 37°C. Microirradiation was performed using an LSM510 confocal microscope (Carl Zeiss). Sensitization of cells was performed by incubating the cells for 20 h in medium containing 2.5 μM deoxyribosylthymine and 0.3 μM bromodeoxyuridine (Sigma), and then staining with 2 μg/mL Hoechst 33258 (Sigma) for 10 min before UVA microirradiation. The 364-nm line of the UVA laser was used for microirradiation (three pulses at 30 μW). Samples were examined with a Zeiss Axioplan 2 equipped with a charge-coupled device camera AxioCam MRm controlled by Axiovision software (Zeiss).

Knockdown experiments

HeLa cells or *STEFKu70*$^{-/-}$*phprt-DR-GFP* cells were transfected with either control siRNA (Silencer Negative Control #1, Ambion 4611), siRNAs for human Tip60 (sc-37966, Santa Cruz Biotechnologies), mouse Tip60-1 (sc-37967, Santa Cruz Biotechnologies), mouse Tip60-2 (D-057795-02-0010, Dharmacon), or RRM1 (GGAUCGCUGUCUCUAA CUUtt) using Lipofectamine 2000 reagent (Invitrogen).

Subcellular fractionation and Mnase treatment

Subcellular fractionation was performed according to a previous report (Mendez and Stillman 2000). The isolated chromatin fraction (1×10^6 cells) was treated with Mnase (15 U) for 30 min at 37°C.

Establishment of STEFKu70$^{-/-}$ *cells containing a phprt-DR-GFP cassette*

The *phprt-DR-GFP* vector (10 μg) was linearized with PvuI and transfected into *STEFKu70*$^{-/-}$ cells. Cells were selected with 1.25 μg/mL puromycin for 12 d, and single colonies were screened by Southern blotting using puromycin cDNA as a probe. Clones having only one copy of the *phprt-DR-GFP* cassette were used for experiments.

Establishment of Tet-on HeLa cells expressing NLS-RC1

pcDNA4/TO-NLS-RC1 (10 μg) was linearized with XhoI and transfected into HeLa T-Rex cells (Invitrogen). Positive clones were selected with Zeocin (250 μg/mL) and Blastcidin (5 μg/mL) for 12 d and screened by immunoblotting using anti-HA antibodies for the detection of NLS-RC1 induction in the presence of tetracycline (1 μg/mL).

Generation of adenoviruses expressing I-SceI endonuclease

The full-length *I-SceI* fragment harboring the *CAG* promoter and poly A signal was subcloned into *pAd/PL-DEST* (Invitrogen). Adenoviruses expressing I-SceI were generated according to the manufacturer's protocol (Invitrogen).

ChIP assay

A population of *STEFKu70*$^{-/-}$ cells (1×10^7) containing *phprt-DR-GFP* cells infected with adenoviruses expressing I-SceI was cross-linked with 1% formaldehyde for 10 min at 37°C. ChIP assays were performed essentially as described (Shimada et al. 2008). Precipitated DNA was resuspended in 50 μL of water and analyzed by quantitative real-time PCR with the ABI PRISM7000 system using Power SYBR Green PCR Master Mix (Applied Biosystems) as described (Katsuno et al. 2009). Primers used for detection of the *I-SceI* break site were indicated in Figure 2A. As an internal control for normalization of the specific fragments amplified, mouse GAPDH locus was amplified using whole genomic DNAs with mGAPDH-F and mGAPDH-R. Primer sequences are supplied in the Supplemental Material.

Comet assay

Alkaline comet assays were performed using a Trevigen's Comet Assay kit (4250-050-k) according to the manufacturer's instructions. DNA was stained with SYBR Green, and slides were photographed digitally (Nikon Eclipse E800 lens and Fuji CCD camera). Tail moments were analyzed as reported previously (Park et al. 2006) using TriTek Comet Score Freeware.

Measurement of DNA damage sensitivity

Tet-on HeLa cells expressing NLS-RC1-HA or NLS-GFP-HA were irradiated with varying doses of IR in the presence or absence of doxycycline (1 μg/mL), and then washed with PBS. Eight days after an additional incubation, surviving colonies were counted, and their relative numbers were expressed as percentages of the untreated cells ($n = 3$).

RNR assay

Insect cells were coinfected with baculoviruses expressing wild-type RRM1 or its mutants, and with those expressing wild-type RRM2. RNR complexes were immunopurified, and their activities were determined according to a method reported previously (Fukushima et al. 2001). Amounts of wild-type RRM1 protein or its mutant proteins were determined by SDS-PAGE and used for calculating specific activities.

Cell cycle synchronization

For synchronization of cells at S phase, knockout–knock-in HeLa cells expressing wild-type or A776CΔ781-C RRM1-HA were first synchronized at the G1/S boundary by exposure to 2.5 mM thymidine for 16 h, and then released into S phase by wash-out of thymidine with PBS and the addition of 20% FBS containing DMEM. Cells were then exposed to IR 3 h after release. For synchronization of cells at G1 phase, knockout–knock-in HeLa cells were synchronized at M phase by exposure to 100 ng/mL nocodazole for 16 h and released into G1 phase by wash-out of nocodazole with PBS and addition of 20% FBS containing DMEM. Cells were then exposed to IR 3 h after release.

Acknowledgments

We thank M. Delhase for critical reading of the manuscript; M. Jasin for hprt-DR-GFP and pCBASce vectors; M. Fukushima for critical advice on the RNR assay; A. Kurimasa for *STEFKu70*$^{-/-}$ MEFs; K. Murata, C. Namikawa-Yamada, and H. Kojima for technical assistance; and M. Inagaki and H. Goto for fluorescence microscopy. This work was supported in part by the Ministry of Education, Science, Sports, and Culture of Japan through Grants-in-Aid for Scientific Research (B) (to M.N.) and (C) (to H.N.), the YASUDA Medical Foundation (to M.N.), and the Sagawa Cancer Foundation (to M.N.).

References

Dong Q, Wang TS. 1995. Mutational studies of human DNA polymerase α. Lysine 950 in the third most conserved region of α-like DNA polymerases is involved in binding the deoxynucleoside triphosphate. *J Biol Chem* **270:** 21563–21570.

Fukushima M, Fujioka A, Uchida J, Nakagawa F, Takechi T. 2001. Thymidylate synthase (TS) and ribonucleotide reductase (RNR) may be involved in acquired resistance to 5-fluorouracil (5-FU) in human cancer xenografts in vivo. *Eur J Cancer* **37:** 1681–1687.

Green CM, Almouzni G. 2003. Local action of the chromatin assembly factor CAF-1 at sites of nucleotide excision repair in vivo. *EMBO J* **22:** 5163–5174.

Guittet O, Hakansson P, Voevodskaya N, Fridd S, Graslund A, Arakawa H, Nakamura Y, Thelander L. 2001. Mammalian p53R2 protein forms an active ribonucleotide reductase in vitro with the R1 protein, which is expressed both in resting cells in response to DNA damage and in proliferating cells. *J Biol Chem* **276:** 40647–40651.

Hakansson P, Hofer A, Thelander L. 2006. Regulation of mammalian ribonucleotide reduction and dNTP pools after DNA damage and in resting cells. *J Biol Chem* **281:** 7834–7841.

Ikura T, Ogryzko VV, Grigoriev M, Groisman R, Wang J, Horikoshi M, Scully R, Qin J, Nakatani Y. 2000. Involvement of the TIP60 histone acetylase complex in DNA repair and apoptosis. *Cell* **102:** 463–473.

Ikura T, Tashiro S, Kakino A, Shima H, Jacob N, Amunugama R, Yoder K, Izumi S, Kuraoka I, Tanaka K, et al. 2007. DNA damage-dependent acetylation and ubiquitination of H2AX enhances chromatin dynamics. *Mol Cell Biol* **27:** 7028–7040.

Imaizumi T, Jean-Louis F, Dubertret ML, Bailly C, Cicurel L, Petchot-Bacque JP, Dubertret L. 1996. Effect of human basic fibroblast growth factor on fibroblast proliferation, cell volume, collagen lattice contraction: In comparison with acidic type. *J Dermatol Sci* **11:** 134–141.

Johnson RE, Trincao J, Aggarwal AK, Prakash S, Prakash L. 2003. Deoxynucleotide triphosphate binding mode conserved in Y family DNA polymerases. *Mol Cell Biol* **23:** 3008–3012.

Katsuno Y, Suzuki A, Sugimura K, Okumura K, Zineldeen DH, Shimada M, Niida H, Mizuno T, Hanaoka F, Nakanishi M. 2009. Cyclin A–Cdk1 regulates the origin firing program in mammalian cells. *Proc Natl Acad Sci* **106:** 3184–3189.

Kraynov VS, Showalter AK, Liu J, Zhong X, Tsai MD. 2000. DNA polymerase β: Contributions of template-positioning and dNTP triphosphate-binding residues to catalysis and fidelity. *Biochemistry* **39:** 16008–16015.

Lee YD, Elledge SJ. 2006. Control of ribonucleotide reductase localization through an anchoring mechanism involving Wtm1. *Genes & Dev* **20:** 334–344.

Lee YD, Wang J, Stubbe J, Elledge SJ. 2008. Dif1 is a DNA-damage-regulated facilitator of nuclear import for ribonucleotide reductase. *Mol Cell* **32:** 70–80.

Mendez J, Stillman B. 2000. Chromatin association of human origin recognition complex, cdc6, and minichromosome maintenance proteins during the cell cycle: Assembly of prereplication complexes in late mitosis. *Mol Cell Biol* **20:** 8602–8612.

Murr R, Loizou JI, Yang YG, Cuenin C, Li H, Wang ZQ, Herceg Z. 2006. Histone acetylation by Trrap–Tip60 modulates loading of repair proteins and repair of DNA double-strand breaks. *Nat Cell Biol* **8:** 91–99.

Niida H, Katsuno Y, Banerjee B, Hande MP, Nakanishi M. 2007. Specific role of Chk1 phosphorylations in cell survival and checkpoint activation. *Mol Cell Biol* **27:** 2572–2581.

Nordlund P, Reichard P. 2006. Ribonucleotide reductases. *Annu Rev Biochem* **75:** 681–706.

Park JH, Park EJ, Lee HS, Kim SJ, Hur SK, Imbalzano AN, Kwon J. 2006. Mammalian SWI/SNF complexes facilitate DNA double-strand break repair by promoting γ-H2AX induction. *EMBO J* **25:** 3986–3997.

Pierce AJ, Hu P, Han M, Ellis N, Jasin M. 2001. Ku DNA end-binding protein modulates homologous repair of double-strand breaks in mammalian cells. *Genes & Dev* **15:** 3237–3242.

Pontarin G, Fijolek A, Pizzo P, Ferraro P, Rampazzo C, Pozzan T, Thelander L, Reichard PA, Bianchi V. 2008. Ribonucleotide reduction is a cytosolic process in mammalian cells independently of DNA damage. *Proc Natl Acad Sci* **105:** 17801–17806.

Reichard P. 1993. From RNA to DNA, why so many ribonucleotide reductases? *Science* **260:** 1773–1777.

Shimada M, Niida H, Zineldeen DH, Tagami H, Tanaka M, Saito H, Nakanishi M. 2008. Chk1 is a histone H3 threonine 11 kinase that regulates DNA damage-induced transcriptional repression. *Cell* **132:** 221–232.

Zhang Z, Yang K, Chen CC, Feser J, Huang M. 2007. Role of the C terminus of the ribonucleotide reductase large subunit in enzyme regeneration and its inhibition by Sml1. *Proc Natl Acad Sci* **104:** 2217–2222.

Biochemical and Biophysical Research Communications 392 (2010) 289–294

Contents lists available at ScienceDirect

Biochemical and Biophysical Research Communications

journal homepage: www.elsevier.com/locate/ybbrc

Anaphase-promoting complex/cyclosome-cdh1 mediates the ubiquitination and degradation of TRB3

Nobumichi Ohoka [a,1], Satoshi Sakai [a], Kikuo Onozaki [a], Makoto Nakanishi [b], Hidetoshi Hayashi [a,*]

[a] Graduate School of Pharmaceutical Sciences, Nagoya City University, 3-1 Tanabe-dori, Mizuho-ku, Nagoya 467-8603, Japan
[b] Graduate School of Medical Sciences, Nagoya City University, 1 Kawasumi, Mizuho-cho, Mizuho-ku, Nagoya 467-8601, Japan

ARTICLE INFO

Article history:
Received 24 December 2009
Available online 11 January 2010

Keywords:
TRB3
APC/C
Cdh1
Proteasome
Degradation

ABSTRACT

We have recently demonstrated that TRB3, a novel endoplasmic reticulum (ER) stress-inducible protein, is induced by CHOP and ATF4 to regulate their function and ER stress-induced cell death; however, the regulation of TRB3 function has not been well characterized. Here we demonstrate that TRB3 is an unstable protein regulated by the ubiquitin–proteasome system. The carboxyl-terminal domain of TRB3 is necessary for protein degradation, and in this region, we found the typical D-box motif, which is a critical sequence for the anaphase-promoting complex/cyclosome (APC/C) dependent proteolysis. TRB3 proteins were stabilized by deletion of its D-box motif and interacted with APC/C coactivator proteins, Cdc20 and Cdh1. The expression level of TRB3 protein is down-regulated by over-expression of Cdh1 but not by that of Cdc20. In addition, knockdown of Cdh1 enhanced the endogenous TRB3 expression level and suppressed its ubiquitination level. These results suggest that APC/C^{Cdh1} is involved in ubiquitination and down-regulating the stability of TRB3 protein.

Introduction

The pseudokinase tribbles 3 (TRB3; also termed SINK, SKIP3, NIPK) is one of the mammalian orthologs of *tribbles*, a cell cycle regulator during development in *Drosophila* [1,2]. TRB3 and other *tribbles* family members (TRB1 and TRB2) contain the classic substrate-binding domains of a protein kinase but not the ATP-binding and kinase-activating domains; therefore, they do not have a kinase activity [3].

TRB3 does not possess a characteristic functional domain (possesses only an incomplete kinase like domain), however, it acts as a multifunctional molecule by interacting with the various proteins. The association of TRB3 to the kinases, such as Akt and MAPK, leads to inhibition of phosphorylation of them [4,5], and the interaction with the transcription factors, such as NF-κB/p65, ATF4, CHOP, C/EBPβ and PPARγ, causes repression of these transcriptional activities [6–11]. On the other hand, TRB3 is also involved in the ubiquitin–proteasome pathway as well as *Drosophila* tribbles by functioning as an adaptor protein for the ubiquitin E3 ligases, thereby promoting the ubiquitination and degradation of acetyl-coenzyme A carboxylase (ACC) and Smurf1 [12,13]. Through these functions, TRB3 has been shown to play an important role in various phenomenon including gluconeogenesis, muscle and adipocyte differentiation, the stress response including hypoxia, anoxia and endoplasmic reticulum (ER) stress, and signal transduction of cytokines containing interleukins and tumor necrosis factor α (TNFα), and bone morphogenetic protein (BMP) [3–15].

It has been reported that the expression of TRB3 is regulated at transcriptional level and mRNA stabilization during fasting condition, differentiation and the stress responses [4,8,10–12,15]. Furthermore, in the past study, the treatment of proteasome inhibitors induced the increase of TRB3 protein expression, suggesting that TRB3 expression level is also modulated by a proteasome-dependent mechanism [13].

Some of the E3 ligases specifically degrade substrate proteins by recognizing the formal amino acid sequences in the target molecules. The D-box motif consists of a consensus sequence of RxxLxxxxN and is recognized by the E3 ligase complexes APC/C containing Cdh1 or Cdc20, and APC/Cs degrade the cell cycle regulators possessing a D-box sequence, such as cyclinB1, Skp2, Aurora-A and Id2, as the target substrates [16–18]. In this study, we found that TRB3 protein contains a D-box motif and is ubiquitinated and degraded by Cdh1 via this motif.

Abbreviations: aa, amino acid; ACC, acetyl-coenzyme A carboxylase; APC/C, anaphase-promoting complex/cyclosome; ATF4, activating transcription factor 4 ; C/EBP, CCAAT/enhancer-binding protein; CHOP, C/EBP homologous protein; E3, ubiquitin-protein isopeptide ligase; ER, endoplasmic reticulum; GFP, green fluorescent protein; PPAR, peroxisome proliferator-activated receptor.

* Corresponding author. Fax: +81 52 836 3484.
E-mail address: hhayashi@phar.nagoya-cu.ac.jp (H. Hayashi).
[1] Present address: Division of Biosignaling, National Institute of Health Sciences, Tokyo 158-8501, Japan.

0006-291X/$ - see front matter © 2010 Elsevier Inc. All rights reserved.
doi:10.1016/j.bbrc.2009.12.175

Materials and methods

Reagents. Dulbecco's modified Eagle's medium, anti-β-actin monoclonal antibody (AC-15), and anti-FLAG monoclonal antibody (M2) were purchased from Sigma. Fetal bovine serum was from HyClone (Logan, UT). MG132 was obtained from Peptide Institute (Osaka, Japan). Cycloheximide was obtained from Nacalai Tesque (Kyoto, Japan). Anti-Cdh1 monoclonal antibody (DH-01) was from Calbiochem (Darmstadt, Germany), and anti-Cdc20 polyclonal antibody (H-175) and anti-Cdc25A polyclonal antibody (M-191) were from Santa Cruz (Santa Cruz, CA). Anti-Myc monoclonal antibody (9E10) was from Roche (Indianapolis, IN). Anti-GFP monoclonal antibody (JL8) was from Clontech (Mountain View, CA). The antiserum against human TRB3 was prepared as described previously [8].

Cell culture. The embryonic kidney cell line 293 and human hepatocellular carcinoma cell line HepG2 were cultured as described previously [19].

Construction of expression plasmids. The plasmids pCMV5-Flag-TRB3, pCMV5-Flag-TRB3ΔN lacking aa 1–127, pCMV5-Flag-TRB3ΔC lacking aa 283–358, pCMV5-Flag-TRB3N179 lacking aa 180–358, pCMV5-Flag-TRB3C179 lacking aa 1–179 or pCMV5-Flag-TRB3ΔAkt lacking aa 239–265, the region essential for the binding with Akt1 of human TRB3 were constructed as described previously [8]. pCMV5-Flag-TRB3ΔD-box lacking aa 195–202 were generated by PCR. pMT-123 (HA-Ub) [20] was kindly provided by Dr. D. Bohmann (University of Rochester Medical Center). pcDNA3-Myc-Cdh1 and pcDNA3-Myc-Cdc20 [21] was kindly provided by Dr. J.M. Peters (Research Institute of Molecular Pathology, Austria). All constructs were verified by sequencing.

Immunoprecipitation and Western blot analysis. Cells were transiently transfected and treated as described in the figure legends. The cells were lysed in RIPA buffer (50 mM Tris–HCl, pH 8.0, 150 mM NaCl, 0.1% SDS, 0.5% deoxycholate, and 1% Triton X-100) supplemented with protease inhibitors. The lysates were subjected to immunoprecipitation, and 1–2% of the lysate or co-immunoprecipitates was subjected to SDS–PAGE (5–12.5%), transferred onto a PVDF membrane and probed with the antibodies indicated in the figure legends. The immunoreactive proteins were visualized using ECL (Amersham Bioscience) or Immobilon (Millipore) Western blotting detection reagents, and light emission was quantified with a LAS1000 lumino image analyzer (FUJI, Japan).

RNA interference. Double stranded RNA duplexes corresponding to human TRB3, Cdh1 and Cdc20 were obtained from Dharmacon Inc. (Chicago, IL).

Transfection. 293 and HepG2 cells were transfected using the Chen-Okayama method as described previously [19]. For RNA interference, HepG2 cells were transfected using a lipofection method with Lipofectamine RNAi MAX (Invitrogen).

Results

TRB3 protein is degraded by ubiquitin–proteasome pathway

To determine the stability of TRB3 protein, we first examined the effects of a proteasome inhibitor MG132 on its ectopic expression. Proteasome inhibition resulted in increased FLAG-TRB3 steady-state protein levels (Fig. 1A), which was accompanied by accumulation of polyubiquitin-reactive signals in the TRB3 immune-complexes (Fig. 1C). We determined the endogenous TRB3 stability in HepG2 cells by blocking *de novo* protein synthesis with cycloheximide and analyzing the remaining TRB3 protein amounts by immunoblotting. TRB3 had a short half-life of approximately 15 min, and this was increased markedly in the presence of MG132, as amounts remained virtually unchanged 60 min after

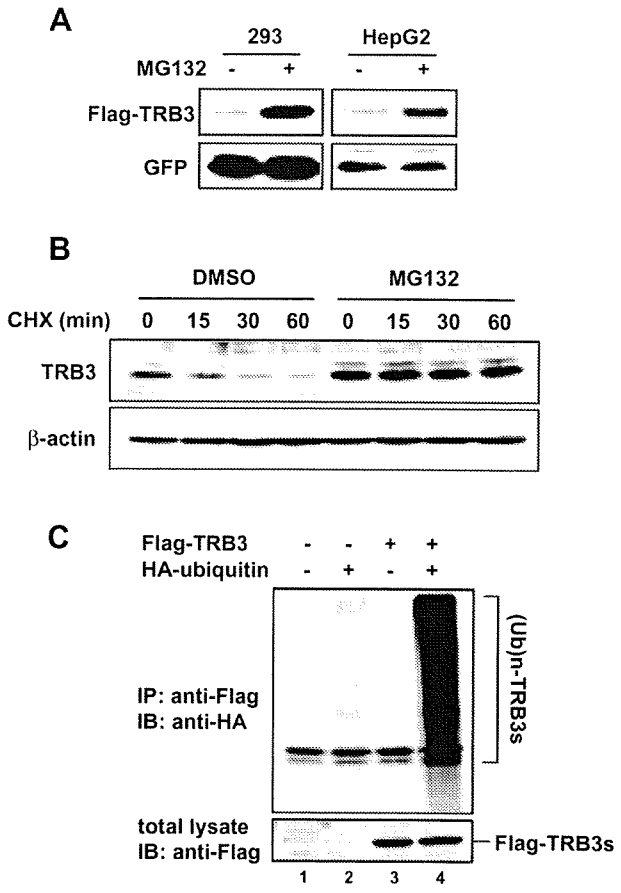

Fig. 1. TRB3 protein is degraded via the ubiquitin–proteasome pathway. (A) 293 and HepG2 cells were transiently transfected with expression vector for Flag-TRB3. After 24 h, the cells were treated with 10 μM MG132 for 12 h. The cell lysates were analyzed by immunoblotting using anti-FLAG antibody. The pEGFP-C1 expression vector was included in each transfection as a transfection efficiency control, and its level was detected with anti-GFP antibody. (B) HepG2 cells were treated with 10 μM MG132 for 6 h and then chased with or without 10 μM MG132 and 10 μg/ml of cycloheximide (CHX) for the indicated periods. The cell lysates were analyzed by immunoblotting using anti-TRB3 and anti-β-actin antibodies. (C) 293 Cells were transiently transfected with the indicated constructs. After 24 h, the cells were treated with 10 μM MG132 for 12 h. The cell lysates were immunoprecipitated with anti-FLAG antibody, and multi-ubiquitinated TRB3 was detected by immunoblotting with anti-HA antibody. The expression level of each protein was assessed by immunoblotting with the indicated antibodies.

cycloheximide treatment (Fig. 1B). These data indicate that TRB3 is regulated by the ubiquitin–proteasome system.

Mapping of the TRB3 region required for its stability

Next we used various TRB3 deletion mutants to map the region responsible for TRB3 stability (Fig. 2A). This experiment demonstrated that the region aa 180–238 and aa 266–282 is crucial in TRB3 degradation. Within this region, a D-box motif was found in TRB3 between residues 195–202 that show a consensus of RxxLxxxxN (Fig. 2B). This motif, targeted by the anaphase-promoting complex/cyclosome (APC/C), is usually found in cell cycle-regulated proteins and mediates degradation of these proteins. To determine whether the D-box is required for the degradation of TRB3, the D-box was deleted, and the resulting TRB3 mutant (ΔD-box) was tested in the pulse-chase assay and the ubiquitination experiment. As shown in Fig. 2C, deletion of this D-box motif (TRB3ΔD-box) increased the stability of TRB3 protein and no enhancement of its accumulation was observed with MG132 treatment. Consistent with this, deletion of the D-box prevented the

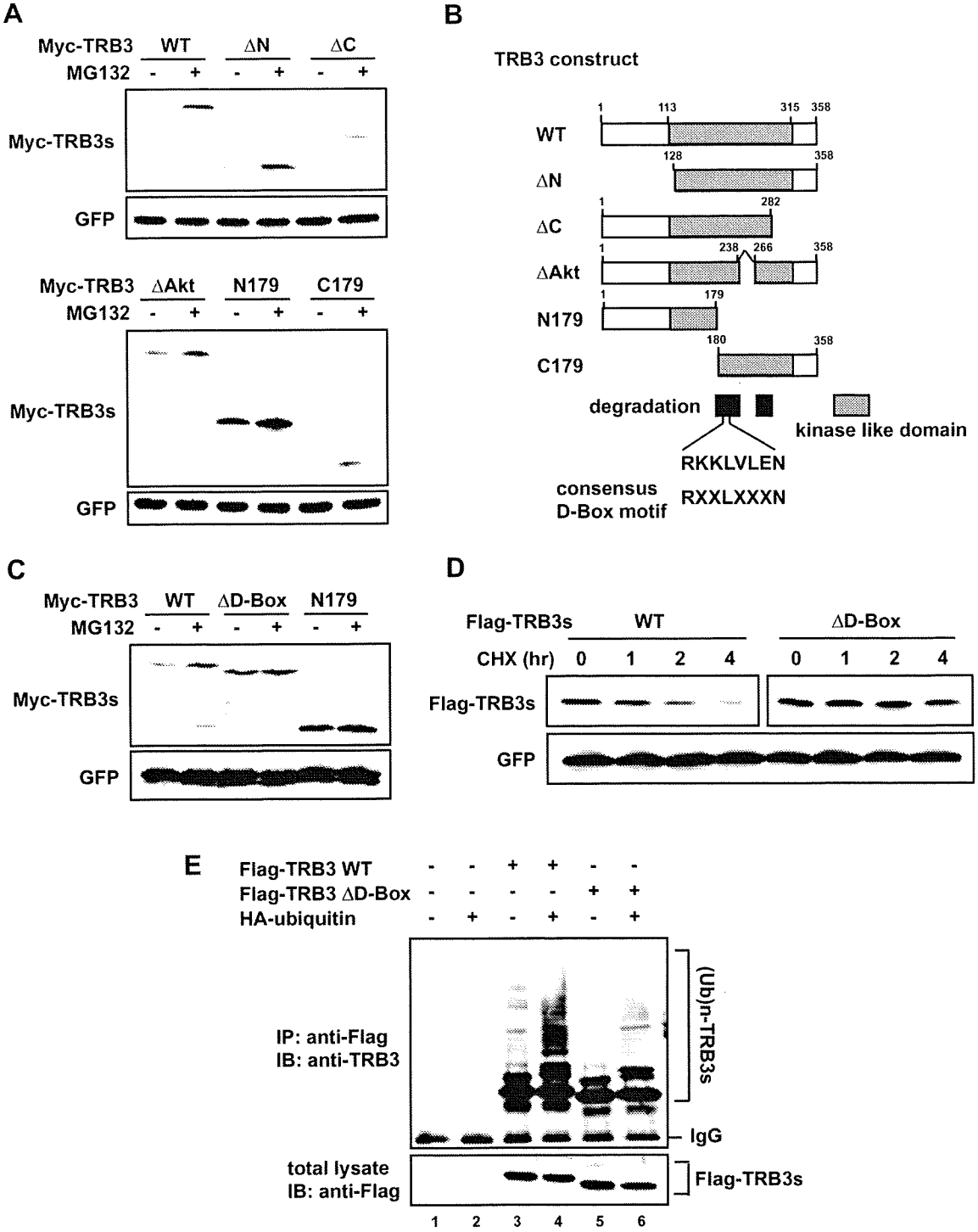

Fig. 2. The D-box motif of TRB3 is critical for its ubiquitination. (A, C) 293 Cells were transiently transfected with expression vector for wild-type Myc-TRB3 or its mutants. After 24 h, the cells were treated with or without 10 μM MG132 for 12 h. The cell lysates were analyzed by immunoblotting using anti-Myc antibody. The pEGFP-C1 expression vector was included in each transfection as a transfection efficiency control, and its level was detected with anti-GFP antibody. (B) The constructs of TRB3 mutants and the amino acids sequence of the D-Box motif in TRB3. (D) 293 Cells were transiently transfected with expression vector for Flag-TRB3 wild type or ΔD-Box. After 36 h, the cells were chased with 10 μg/ml of cycloheximide (CHX) for the indicated periods. The cell lysates were analyzed by immunoblotting using anti-FLAG and anti-GFP antibodies. (E) 293 Cells were transiently transfected with the indicated constructs. After 24 h, the cells were treated with 10 μM MG132 for 12 h. The cell lysates were immunoprecipitated with anti-FLAG antibody, and multi-ubiquitinated TRB3s were detected by immunoblotting with anti-TRB3 antibody. The expression level of each protein was assessed by immunoblotting with the indicated antibodies.

ubiquitination and degradation of TRB3 (Fig. 2D and E). Thus, the D-box is essential for degradation of TRB3, and a ubiquitin ligase complex that targets the D-box, possibly the APC/C, is required for the degradation of TRB3.

TRB3 interacts with APC/C coactivators, Cdc20 and Cdh1

APC/C critically requires either one of two WD40-domain proteins, Cdc20 or Cdh1, as activators. These activators interact

dynamically with the APC/C and may either facilitate recruitment of substrates by their WD40 domains, or enhance the specific activity of the APC/C. To examine whether Cdc20 or Cdh1 can interact with TRB3 through its D-box, cell extract was prepared from 293 cells co-expressed with Flag-TRB3 and Myc-Cdc20 or Myc-Cdh1. TRB3 was found to interact with both Cdh1 and Cdc20 (Fig. 3A). We also found that endogenous TRB3 also co-immunoprecipitated efficiently with endogenous Cdh1 (Fig. 3B).

Cdh1 regulates TRB3 steady-state levels

To investigate whether two activators are involved in the TRB3 instability, FLAG-TRB3 was ectopically co-expressed with Cdh1 or Cdc20 in 293 cells. As shown in Fig. 4A, Cdh1 markedly decreased the TRB3 expression, but Cdc20 did not. This effect was fully recovered by MG132 (Fig. 4B). TRB3 protein lacking D-box motif was resistant to Cdh1-mediated degradation (Fig. 4C).

We also investigated whether Cdh1 depletion affects the TRB3 protein stability (Fig. 4D). Cdh1 silencing by small interfering RNA (siRNA) in HepG2 cells resulted in increased TRB3 steady-state levels. Cdh1 knockdown also induced the accumulation of Cdc20 and Cdc25A, known as targets of APC/C^{Cdh1}. When Cdc20 was knock downed, no accumulation of TRB3 was observed. We have reported that endoplasmic reticulum stress induced the TRB3 expression in a CHOP dependent manner [8], however Cdh1 ablation caused the accumulation of TRB3 without any CHOP induction (Fig. 4E). Consistent with these data, Cdh1 depletion effectively suppressed the TRB3 ubiquitination at steady-state (Fig. 4F). Taken together, these findings indicate that APC/C^{Cdh1} regulates the TRB3 steady-state levels.

Interestingly, TRB3 silencing caused both Cdc20 and Cdc25A accumulation without any change of Cdh1 expression level (Fig. 4D, lane 4), suggesting that TRB3 has some influence on the Cdh1 dependent degradation.

Discussion

TRB3 is induced by an ATF4/CHOP dependent manner in the various stressful conditions and regulated the stabilities and functions of ATF4/CHOP [7–9]. However, the mechanism underlying TRB3 regulation has been unclear. Our results demonstrated that TRB3 is a short-lived protein and its steady-state levels are balanced through proteasome-dependent degradation, which is facilitated by Cdh1, one of the activators of ubiquitin ligase APC/C. APC/C is a key ubiquitin ligase complex, which regulates the progression of the cell cycle by control the ubiquitination and subsequent degradation of a number of core cell cycle regulators. APC/C activity is controlled mainly through the regulated binding of two co-activators, Cdc20 and Cdh1, which target distinct substrates at specific stages during the cell cycle.

TRB3 has the typical D-box destruction motif, which is a critical sequence containing in substrates for the APC/C^{Cdc20} and APC/C^{Cdh1} dependent proteolysis. No KEN-box motif, which is additionally recognized by APC/C^{Cdh1} was existed in TRB3. We observed that both Cdh1 and Cdc20 interacted with TRB3, but that APC/C^{Cdh1} alone contributed the TRB3 stability.

During anaphase, Cdh1 was activated by interacting with APC/C complex to form APC/C^{Cdh1}, which continues to ubiquitinate mitotic cyclins along with new targets, including Cdc20, driving cells out of mitosis into G_0/G_1 phase. APC/C^{Cdh1} activity persists throughout G_1 phase until Cdh1 is inactivated at the G_1 to S transition through degradation, phosphorylation and binding of Emi1. TRB3 is considered as a pseudokinase, which contains the typical substrate-binding domains, but lack the ATP-binding and kinase-activation domains [3], and it could be a novel type of endogenous kinase inhibitor, acting as a decoy kinase-like protein for modulating the cell cycle. Expression level of TRB3 could be regulated in a cell cycle dependent manner according to the APC/C^{Cdh1} activity to modulate the activities of key kinases for the cell cycle.

We found that the Cdh1 expression level was not affected by TRB3 deletion (Fig. 4D) or over-expression (data not shown), however, TRB3 deletion up-regulated the expression levels of Cdc20 and Cdc25A, both of which are targets for APC/C^{Cdh1}. These results indicate that TRB3 may regulate the APC/C^{Cdh1} activity.

Multiple primary human lung, colon, and breast tumors express high levels of TRB3 transcript [3,22]. Consistently, several studies have reported reduced expression of Cdh1 in human tumors [23]. In fact, Cdh1 heterozygous animals show increased susceptibility to spontaneous tumors, suggesting that Cdh1 functions as a tumor suppressor by preventing genomic instability [24]. It is possible that TRB3 over-expressed in multiple human tumors and tumor-derived cell lines is caused by not only augmented transcription induced by various stresses but also the stabilization of its protein through the down-regulation of APC/C^{Cdh1}. Further study is necessary to clarify whether over-expressed TRB3 contributes to tumorigenesis.

Recently another type of E3 ubiquitin ligase, seven in absentia homolog 1 (SIAH1) was reported to be involved in the ubiquitination and degradation of TRB3 [25]. Siah is induced by p53, response to genotoxic stress to destruct β-catenin, contributing to cell cycle arrest [26]. Genotoxic stress was reported to downregulate TRB3 expression [27]. Stability of TRB3 is regulated by at least two kinds

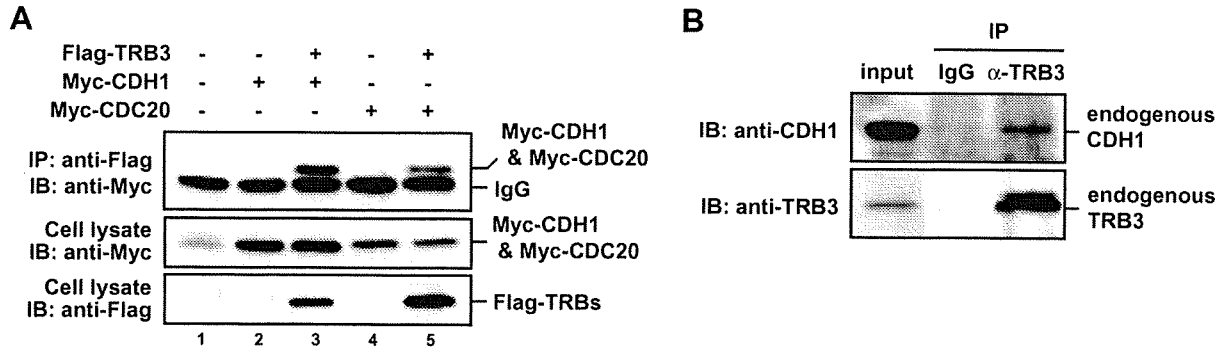

Fig. 3. TRB3 physically interacts with Cdh1. (A) 293 Cells were transiently transfected with the indicated constructs After 24 h, the cells were treated with 10 μM MG132 for 12 h. The cell lysates were immunoprecipitated with anti-FLAG antibody, and immunoblotting of cell lysates was performed with anti-FLAG or anti-Myc antibodies. The expression level of each protein was assessed by the immunoblotting of the cell lysates with the indicated antibodies. (B) HepG2 cells were treated with 10 μM MG132 for 8 h. The cell lysates were immunoprecipitated with anti-TRB3 antibody or control IgG and immunoblotted with anti-Cdh1 or anti-TRB3 antibodies. The expression level of each protein was assessed by immunoblotting with the indicated antibodies.

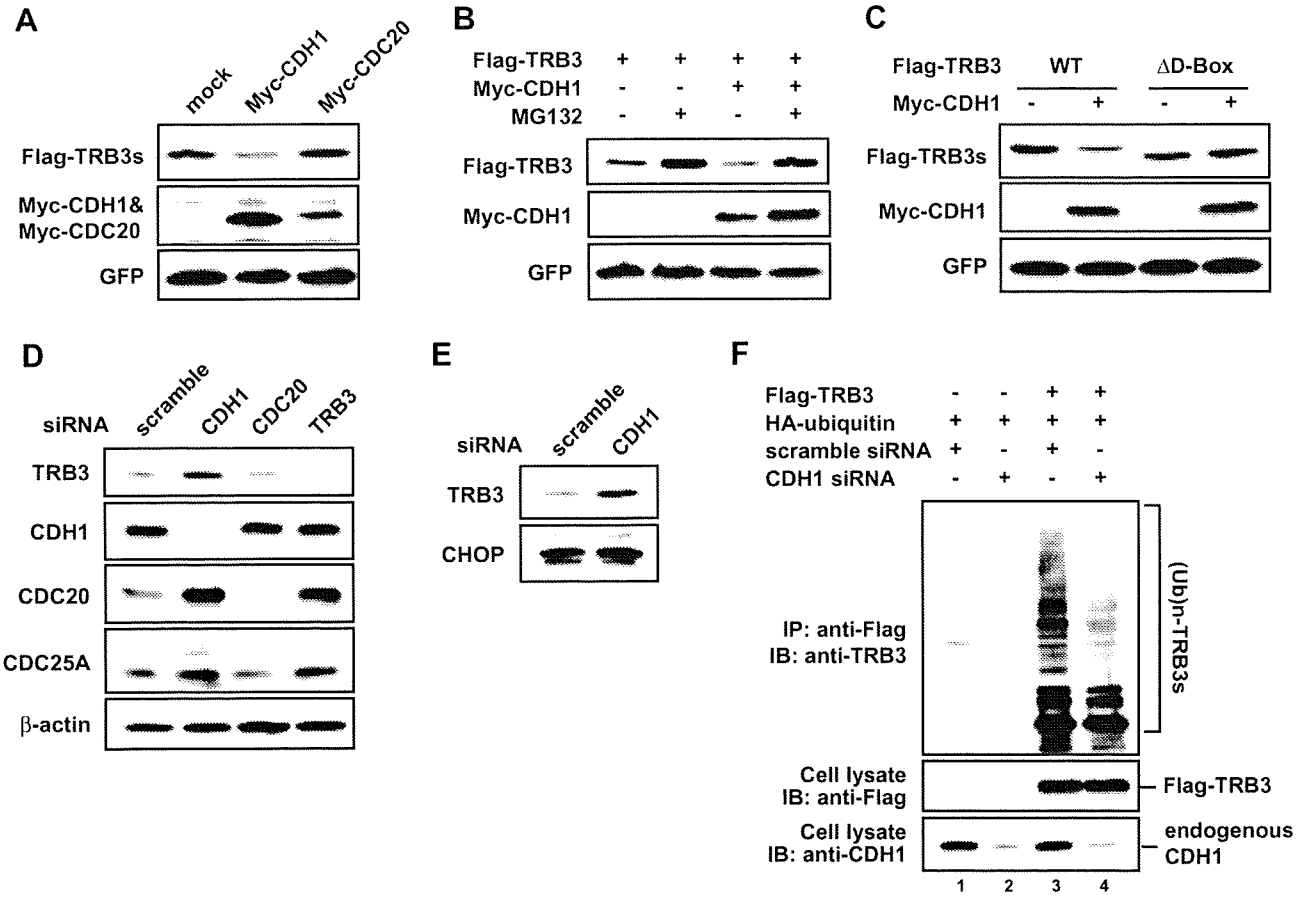

Fig. 4. Cdh1 ubiquitinates and degrades TRB3 protein via its D-box motif. (A–C) 293 Cells were transiently transfected with the indicated constructs. After 24 h, the cells were treated (B) or untreated (A, C) with 10 μM MG132 for 12 h. The cell lysates were analyzed by immunoblotting using anti-FLAG or anti-Myc antibodies. The pEGFP-C1 expression vector was included in each transfection as a transfection efficiency control, and its level was detected with anti-GFP antibody. (D, E) HepG2 cells were transiently transfected with control (scramble) siRNA or indicated siRNA. After 48 h, the cell lysates were analyzed by immunoblotting using the indicated antibodies. (F) 293 Cells were transiently transfected with the indicated constructs and control (scramble) or Cdh1 siRNA. After 24 h, the cells were treated with 10 μM MG132 for 12 h. The cell lysates were immunoprecipitated with anti-FLAG antibody, and multi-ubiquitinated TRB3s were detected by immunoblotting with anti-TRB3 antibody. The expression level of each protein was assessed by immunoblotting with the indicated antibodies.

of E3 ligases, APC/C^{Cdh1} and SIAH1, and these ligases would be used properly by the situation of cells; APC/C^{Cdh1} is used at the steady-state and SIAH1 response to genotoxic stress.

In summary, this study provides that the TRB3 expression is regulated by its protein degradation as well as at the transcriptional level. Important roles of the Cdh1-dependent form of the APC/C on the TRB3 stability implicate its additional function in cell cycle besides the recently described roles in and in the stress response. These results allowed us to investigate the role of cell cycle of TRB3.

Acknowledgments

We are grateful to thank Dr. Dirk Bohmann and Dr. Jan-Michael Peters for providing expression plasmids. This research was supported in part by a grant-in-aid for Scientific Research (C) from Japan Society for the Promotion of Science, and grants-in-aid for Scientific Research on Priority Areas from The Ministry of Education, Science, Sports and Culture, and Grants-in-Aid for Scientific Research from Nagoya City University.

References

[1] J. Grosshans, E. Wieschaus, A genetic link between morphogenesis and cell division during formation of the ventral furrow in *Drosophila*, Cell 101 (2000) 523–531.
[2] J. Mata, S. Curado, A. Ephrussi, P. Rorth, Tribbles coordinates mitosis and morphogenesis in *Drosophila* by regulating string/CDC25 proteolysis, Cell 101 (2000) 511–522.
[3] A.J. Bowers, S. Scully, J.F. Boylan, SKIP3, novel *Drosophila* tribbles ortholog, is overexpressed in human tumors and is regulated by hypoxia, Oncogene 22 (2003) 2823–2835.
[4] K. Du, S. Herzig, R.N. Kulkarni, M. Montminy, TRB3: a tribbles homolog that inhibits Akt/PKB activation by insulin in liver, Science 300 (2003) 1574–1577.
[5] E. Kiss-Toth, S.M. Bagstaff, H.Y. Sung, V. Jozsa, C. Dempsey, J.C. Caunt, K.M. Oxley, D.H. Wyllie, T. Polgar, M. Harte, L.A. O'neill, E.E. Qwarnstrom, S.K. Dower, Human tribbles, a protein family controlling mitogen-activated protein kinase cascades, J. Biol. Chem. 279 (2004) 42703–42708.
[6] M. Wu, L.G. Xu, Z. Zhai, H.B. Shu, SINK is a p65-interacting negative regulator of NF-κB-dependent transcription, J. Biol. Chem. 278 (2003) 27072–27079.
[7] D. Ord, T. Ord, Mouse NIPK interacts with ATF4 and affects its transcriptional activity, Exp. Cell Res. 286 (2003) 308–320.
[8] N. Ohoka, S. Yoshii, T. Hattori, K. Onozaki, H. Hayashi, TRB3, a novel ER stress-inducible gene, is induced via ATF4-CHOP pathway and is involved in cell death, EMBO J. 24 (2005) 1243–1255.
[9] N. Ohoka, T. Hattori, M. Kitagawa, K. Onozaki, H. Hayashi, Critical and functional regulation of CHOP (C/EBP homologous protein) through the N-terminal portion, J. Biol. Chem. 282 (2007) 35687–35694.
[10] O. Bezy, C. Vernochet, S. Gesta, S.R. Farmer, C.R. Kahn, TRB3 blocks adipocyte differentiation through the inhibition of C/EBPβ transcriptional activity, Mol. Cell. Biol. 27 (2007) 6818–6831.
[11] Y. Takahashi, N. Ohoka, H. Hayashi, R. Sato, TRB3 suppresses adipocyte differentiation by negatively regulating PPARγ transcriptional activity, J. Lipid Res. 49 (2008) 880–892.
[12] L. Qi, J.E. Heredia, J.Y. Altarejos, R. Screaton, N. Goebel, S. Niessen, I.X. Macleod, C.W. Liew, R.N. Kulkarni, J. Bain, C. Newgard, M. Nelson, R.M. Evans, J. Yates, M. Montminy, TRB3 links the E3 ubiquitin ligase COP1 to lipid metabolism, Science 312 (2006) 1763–1766.

[13] M.C. Chan, P.H. Nguyen, B.N. Davis, N. Ohoka, H. Hayashi, K. Du, G. Lagna, A. Hata, Mol. Cell. Biol. 27 (2007) 5776–5789.
[14] S. Kato, K. Du, TRB3 modulates C2C12 differentiation by interfering with Akt activation, Biochem. Biophys. Res. Commun. 354 (2007) 933–938.
[15] T. Rzymski, A. Paantjens, J. Bod, A.L. Harris, Multiple pathways are involved in the anoxia response of SKIP3 including HuR-regulated RNA stability, NF-κB and ATF4, Oncogene 27 (2008) 4532–4543.
[16] W. Wei, N.G. Ayad, Y. Wan, G.J. Zhang, M.W. Kirschner, W.G. Kaelin Jr., Degradation of the SCF component Skp2 in cell-cycle phase G1 by the anaphase-promoting complex, Nature 428 (2004) 194–198.
[17] Y. Arlot-Bonnemains, A. Klotzbucher, R. Giet, R. Bihan, C. Prigent, Identification of a functional destruction box in the Xenopus laevis aurora-A kinase pEg2, FEBS Lett. 508 (2001) 149–152.
[18] A.G. Liu, M.S. Carro, G. Rothschild, L. de la Torre-Ubieta, M. Pagano, A. Bonni, A. Iavarone, Degradation of Id2 by the anaphase-promoting complex couples cell cycle exit and axonal growth, Nature 442 (2006) 471–474.
[19] T. Hattori, N. Ohoka, Y. Inoue, H. Hayashi, K. Onozaki, C/EBP family transcription factors are degraded by the proteasome but stabilized by forming dimmer, Oncogene 22 (2003) 1273–1280.
[20] M. Treier, L.M. Staszewski, D. Bohmann, Ubiquitin-dependent c-Jun degradation in vivo is mediated by the δ domain, Cell 78 (1994) 787–798.
[21] E.R. Kramer, N. Scheuringer, A.V. Podtelejnikov, M. Mann, J.M. Peters, Mitotic regulation of the APC activator proteins CDC20 and CDH1, Mol. Biol. Cell 11 (2000) 1555–1569.
[22] J. Xu, S. Lv, Y. Qin, F. Shu, Y. Xu, J. Chen, B.E. Xu, X. Sun, J. Wu, TRB3 interacts with CtIP and is overexpressed in certain cancers, Biochim. Biophys. Acta 1770 (2007) 273–278.
[23] J.R. Skaar, M. Pagano, Cdh1: a master G0/G1 regulator, Nat. Cell Biol. 10 (2008) 755–757.
[24] I. García-Higuera, E. Manchado, P. Dubus, M. Cañamero, J. Méndez, S. Moreno, M. Malumbres, Genomic stability and tumour suppression by the APC/C cofactor Cdh1, Nat. Cell Biol. 10 (2008) 802–811.
[25] Y. Zhou, L. Li, Q. Liu, G. Xing, X. Kuai, J. Sun, X. Yin, J. Wang, L. Zhang, F. He, E3 ubiquitin ligase SIAH1 mediates ubiquitination and degradation of TRB3, Cell. Signal. 20 (2008) 942–948.
[26] S. Matsuzawa, J.C. Reed, Siah-1, SIP, and Ebi collaborate in a novel pathway for β-catenin degradation linked to p53 responses, Mol. Cell 7 (2001) 915–926.
[27] C.A. Corcoran, X. Luo, Q. He, C. Jiang, Y. Huang, M.S. Sheikh, Genotoxic and endoplasmic reticulum stresses differentially regulate TRB3 expression, Cancer Biol. Ther. 4 (2005) 1063–1067.

Chromosome Research (2010) 18:103–113
DOI 10.1007/s10577-009-9086-2

Chk1–cyclin A/Cdk1 axis regulates origin firing programs in mammals

Makoto Nakanishi · Yuko Katsuno · Hiroyuki Niida · Hiroshi Murakami · Midori Shimada

Published online: 15 December 2009

Abstract DNA replication is key to ensuring the complete duplication of genomic DNA prior to mitosis and is tightly regulated by both cell cycle machinery and checkpoint signals. Regulation of the S phase program occurs at several stages, affecting origin firing, replication fork elongation, fork velocity, and fork stability, all of which are dependent on S-phase-promoting kinase activity. Somatic mammalian cells use well-established origin programs by which specific regions of the genome are replicated at precise times. However, the mechanisms by which S phase kinases regulate origin firing in mammals are largely unknown. Here, we discuss recent advances in the understanding of how S phase programs are regulated in mammals at the correct regions and at the appropriate times.

Keywords DNA replication · S phase program · cyclin · cyclin dependent kinase (CDK) · checkpoint protein 1 (Chk1)

Abbreviations

ATR	AT and Rad3-related
ATRIP	ATR-Interacting Protein
ATM	Ataxia-Telangiectasia-Mutated
BRCT	BRCA1 C Terminus
CIdU	Chlorodeoxyuridine
DSBs	Double Strand Breaks
GCN5	General Control Nonrepressed 5
IdU	Iododeoxyuridine
Mcm	Minichromosome maintenance
MEFs	Mouse Embryonic Fibroblasts
PIKK	PI3 Kinase-related Kinases
RPA	Replication Protein A
Tip60	Tat-interactive protein, 60 kDa
TopBP1	Topoisomerase Binding Protein 1
β-TRCP	β-Transducin Repeat-Containing Protein 1

Responsible Editors: Marie-Noëlle Prioleau and Dean Jackson.

M. Nakanishi (✉) · Y. Katsuno · H. Niida · H. Murakami · M. Shimada
Department of Cell Biology,
Graduate School of Medical Sciences,
Nagoya City University,
1 Kawasumi, Mizuho-cho, Mizuho-ku,
Nagoya 467-8601, Japan
e-mail: mkt-naka@med.nagoya-cu.ac.jp

Introduction

Duplication of the eukaryotic genome is regulated at multiple stages including the initiation of DNA replication and the origin firing program as well as during replication fork progression and in the control of fork velocity. DNA replication in mammals is initiated at a great number of origins throughout the genome. Mammalian DNA replication is characterized by a high order of uncertainty due to the existence on the genome of hundreds to thousands of potential origins that fire with varying efficiencies and at different times. However, spatial and temporal patterns of DNA replication in mammals are relatively well defined, and distinct patterns of replication foci appear as cells progress from early to late S phase

(Jackson 1995). A single replication factory is actually comprised of several candidate origins, most of which are not normally used since firing of one origin inhibits activation of any other Mcm2-7 complex within the same factory (Woodward et al. 2006). Thus, S phase programs appear to be mediated in two distinct ways; one via the activation of replicon clusters and the other, through the selection of one Mcm2-7 complex within a single replicon.

According to the replicon model, DNA replication is regulated through interaction between cis-acting sequences termed replicators and trans-acting initiation factors known as initiators. With trans-factors, for example, initiation of early origin firing is regulated by cyclin A- or cyclin E-associated Cdk2 activities in normal somatic cells. In addition, Cdc7 activity is also reported to be involved in the regulation of S phase entry. These two kinases are involved in the loading on origins of Cdc45 by phosphorylating subunits of Mcm2-7 complex (Machida et al. 2005). In budding yeast, Cdk phosphorylation of an initiation factor, Sld2/Drc1, is also critical for the initiation of DNA replication (Masumoto et al. 2002). In contrast to those involved in early origin firing, trans-factors that regulate late origin firing have been less clearly identified, although Clb5-dependent Cdk activity is known to be indispensable for activation of late replication origins in budding yeast (Donaldson et al. 1998; Noguchi et al. 2002). These results suggest the existence of a specific trans-factor(s) for late origin activation as there is for early origin. Therefore, our primary aim in this review is to focus on recent findings regarding late origin firing in eukaryotes while emphasizing the components and events that are specific to metazoans.

PIKK kinases are essential for proper timing of late origin replication firing

Although DNA replication is initiated at specific sequence elements in prokaryotes or budding yeast (Stinchcomb et al. 1979), such sequence-specific initiation does not appear to be required in metazoans (DePamphilis 2003). Instead, origin firing is likely dependent on stochastic initiation at dormant origins defined as such be their chromatin status (Gilbert 2004), despite the presence of some origins that are sequence specific (Huberman 1998). Stochastic initiation is organized by feedback regulation from active replicons, which is mediated by the sensing of ongoing replication (Ge et al. 2007; Ibarra et al. 2008). In the *Xenopus laevis* egg system, these ongoing replication events appear to be sensed by the DNA-damage checkpoint kinases ataxia telangiectasia mutated (ATM) and/or AT and Rad3 related (ATR) because inhibition of ATM and ATR with caffeine or specific neutralizing antibodies promoted rapid and synchronous origin firing (Shechter et al. 2004). ATM and ATR kinases are both extremely large proteins that phosphorylate a great number of substrates. Patients bearing an *ATM* mutation suffer from a devastating syndrome called ataxia telangiectasia that causes immunodeficiency, genomic instability, clinical radiosensitivity, and a predisposition to cancer (Shiloh 1997). Although cells lacking ATM are viable, suggesting that *ATM* is a non-essential gene for normal cell cycle progression and development, its kinase activity is strongly stimulated by double strand breaks (DSBs). The identification of a damage-induced phosphorylation site (Ser1981) revealed a new mechanism for ATM regulation by which a rapid and sensitive switch for checkpoint signaling is permitted (Bakkenist and Kastan 2003). ATM under unperturbed conditions exists as a homodimer complex with its kinase active site physically blocked by tight intermolecular binding to a protein domain around Ser1981. In response to DSBs, a conformational change in the ATM protein stimulates it to auto-phosphorylate Ser1981 in an intermolecular manner. In contrast, the auto-phosphorylation of ATM at Ser1981 is suppressed under unperturbed conditions by a constitutive interaction with PP2A that dephosphorylates Ser1981 (Goodarzi et al. 2004). Acetylation of ATM by Tip60 is also reported to be important for its full activation (Sun et al. 2005).

ATR was discovered from its sequence similarity to ATM and Rad3, and was shown to play an essential role in DNA damage and DNA replication checkpoint activation. Mutations in the ATR gene have been reported in a subset of patients with Seckel syndrome (O'Driscoll et al. 2003), which is a human autosomal recessive disorder causing severe intrauterine growth retardation, proportionate dwarfism, microcephaly, with skeletal and brain abnormalities, and a predisposition to cancer. ATR constitutively forms a heterodimer with ATRIP that binds to UV-damaged DNA or to replication protein A (RPA)-coated single-stranded DNA (Zou and